https://doi.org/10.2352/CIC.2024.32.1.21

Adaptive Chroma Correction of Tone Mapping Operators for Natural Image Appearance

Imran Mehmood, Muhammad Usman Khan and Ming Ronnier Luo; State Key Laboratory of Extreme Photonics and Instrumentation, Zhejiang University, Hangzhou, China.

Abstract

Preserving perceptual quality of the tone mapped images is one of the major challenges in tone mapping. Most traditional tone mapping operators (TMOs) compress the luminance of high dynamic range (HDR) images without taking account of image color information, resulting into less natural or preferable colors. Current color management algorithms require either manual fine-tuning or introduce lightness and hue shifts. An adaptive color correction model is proposed to address color distortions in tone mapping. It is based on the CIECAM16 to compute perceptual correlates, i.e., Lightness, Chroma and Hue. Regardless of the tone mapping technique, the proposed model recovers natural colors of tone mapped images for spatially invariant and variant operators, making it an effective postprocessing technique for color reproduction. Unlike other models, it requires no gamut mapping correction, reproducing more accurate hue, chroma, and lightness. The algorithm was evaluated using objective and subjective methods, revealing that it produced significantly better color reproduction for tone mapped images in terms of naturalness of the colors.

Introduction

The HDR representation offers an unlimited tonal range and prioritizes the preservation of fine details [1]. It allows for a more immersive visual experience when viewing movies, taking photographs, playing computer games, or inspecting visualizations [2]. However, most current display devices are not equipped to handle such rich visual content. This is where a TMO comes in, which adjusts the tonal range of HDR data to match the capabilities of the display device.

In the process of tone mapping, color distortions such as incorrect hues, saturations, or brightness levels occur leading to low perceptual quality in terms of unnatural or unattractive images. For instance, consider a high dynamic range image with colors from bright reds to deep blues. The reds and blues are well separated and easily distinguishable in real scenes. However, when the HDR image undergoes tone mapping, the tonal range reduction may cause the reds and blues to become closer in hue, leading to a loss of color distinction (refer to Figure 1). It can result in the reds appearing more orange, the blues appearing more purple, or the overall image appearing more washed out. It can be noticed in Figure 1 (a)-(d), Li TMO [3] produced an overly saturated image, Liang TMO [4] changed the hue of the image, Hui TMO [5] also suffered from saturation and hue changes while Meylan [6] TMO overlay desaturated the tone mapped image.

Most color adjustment schemes are based on manual adjustments of parameters per image and tone mapper, such as Schlick's nonlinear saturation model [7] and Mantiuk's Linear model [8]. Schlick's model introduces lightness shifts, while Mantiuk's model introduces hue shifts, apart from the manual adjustment of parameters. Mantiuk proposed automatic selection of the saturation parameter in linear and nonlinear models by

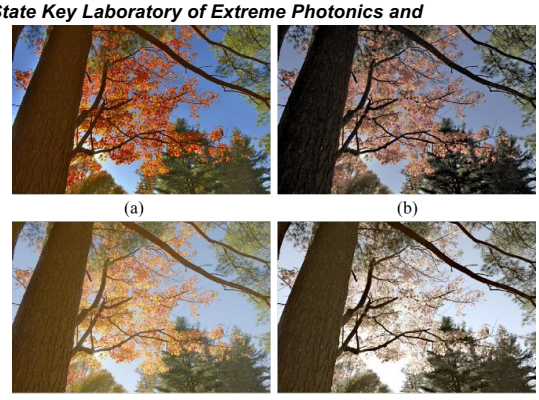

***Figure 1**. Color distortions caused by various TMOs. (a) Li's TMO, (b) Liang's TMO (c) Hui's TMO and (d) Meylan's TMO.*

conducting psychophysical experiments; however, these models are limited to the spatially invariant TMOs [8]. The models do not reproduce the colors appropriately for spatially variant operators since the parameter prediction involves derivatives of the contrast mapping function, and the regions where contrast changes are very high become unnecessarily desaturated. If the hue in the images is distorted, these models do not correct it; instead, Mantiuk's models introduce the hue shifts.

Artusi [9] proposed an automatic saturation adjustment for tone mapped images by scaling the chroma in ICh color space by ratios of the tone mapped image intensity and chroma with the HDR image intensity and chroma, respectively. It introduces lightness shifts. However, the scope of a TMO is to compress the contrast, and the aim of color correction as a post-processing step is specifically to correct the colors without altering the lightness of the original tone mapped image. In the method, gamut correction is needed as the chroma is scaled by the intensity and chroma ratios. The chroma is desaturated to correct out-of-gamut pixels resulting in less optimal colors. If the desaturation step is not applied, hue shifts occur due to out-of-gamut pixels. Hence, in Artusi method, either hue shifts occur or the chroma is less optimal. Moreover, the method overly desaturates tone mapped images for the abovementioned reasons.

The human eye is strongly influenced by its viewing conditions. The luminance and colorimetry information of the light source play critical roles in visual adaptation. Color appearance models (CAMs) such as CIECAM02 [10], CIECAM16 [11] and ZCAM [12] are essential in understanding these mechanisms. They operate through processes that includes chromatic adaptation and tone compression. The models accurately predict various visual effects including Hunt's and Steven's effects. The input parameters to the CAMs are surround conditions and the stimulus, and the output parameters include color appearance attributes including lightness, chroma and hue.

This paper introduces an efficient and effective color postprocessing technique based on the CIECAM16 to compute perceptual correlates. The lightness of the tone mapped image is computed using CIECAM16 and the surround conditions of the tone mapped image. Afterward, the hue and chroma are computed under display conditions from the HDR image by employing tone

mapped image lightness and CIECAM16 color adaptation equations. The proposed model recovers natural colors regardless of the tone mapping technique as the CAMs are developed based on psychophysical experiments to predict the natural appearance of the attributes. Furthermore, this approach does not require any gamut mapping correction algorithms, facilitating optimal color reproduction with ease.

Proposed Model

The color correction model (CCM) requires both a tonemapped image I_t and its corresponding original HDR image I_H, without any processing, to compute the hue and chroma that the model aims to reproduce. Both images must be in the linear RGB color space. HDR images typically exist in the linear domain, but accurate radiometric values are often unavailable, making luminance values inherently relative. The XYZ value (X_T, Y_T, Z_T) of the tone mapped image (R_T, G_T, B_T) may be obtained by using sRGB to XYZ conversion matrix or if the image is present in other color space then the specific color conversion matrix must be applied.

The proposed color correction model (CC_Z) aims to reproduce the hue and chroma from the HDR image while preserving the lightness of the tone-mapped image. The workflow for the CC_Z, depicted in Figure 2, uses CIECAM16 and requires specific surround and display conditions to compute color adaptations. Surround conditions may differ for the tonemapped image and the final display image. There are two types of surround conditions used in the algorithm: 1) to compute the lightness of the tone mapped image, using the adaptation luminance L_{aT}, background luminance Y_{bT} and, white point [X_{wT}, Y_{wT}, Z_{wT}] and 2) to compute the hue and color adaptation from the HDR image under display conditions, using the adaptation luminance L_{ad}, background luminance Y_{bd} and white point [X_{wd}, Y_{wd}, Z_{wd}].

The algorithm begins by calculating the lightness of the tone-mapped image and then adapts the colors from the HDR image, as detailed in subsequent sections. The lightness calculation of the tone-mapped image using CIECAM16 follows a typical workflow. Since the colors are adapted from the HDR image, detailed equations for each step are provided to ensure clarity and prevent misapprehensions.

Lightness Calculation

To determine the lightness of the tone-mapped images, first calculate the achromatic response A_{wT} corresponding to the tone-mapped image white point [X_{wT}, Y_{wT}, Z_{wT}], and the achromatic response of tone-mapped image A_T. Since the image is tone-mapped, the surround conditions related to the tone mapped image are to be used, i.e., L_{AT} and Y_{bT}. Calculate the input parameters of CIECAM16 color appearance model using tone mapped image white point (X_{wT}, Y_{wT}, Z_{wT}) as follows.

$$\begin{pmatrix} R_{wT} \\ G_{wT} \\ B_{wT} \end{pmatrix} = M_{CAT16} \begin{pmatrix} X_{wT} \\ Y_{wT} \\ Z_{wT} \end{pmatrix} \quad (1)$$

Calculate the degree of adaptation, D_T.

$$D_T = F\left[1 - \left(\frac{1}{3.6}\right) exp\left(\frac{-L_{AT}-42}{92}\right)\right] \quad (2)$$

Calculate other parameters.

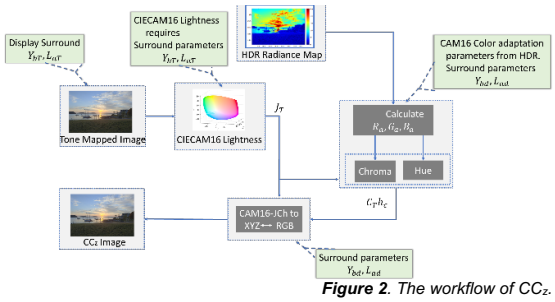

***Figure 2**. The workflow of CC_Z.*

$D_R = D_{RY_{WT}W_T} + 1 - D_T$, $D_G = D_{GY_{WT}W_T} + 1 - D_T$, $D_B = D_{BY_{WT}W_T} +$

$1 - D_T$ (3)

$F_{LT} = 0.2k_4(5L_{AT}) + 0.1(1 - k_{4T})_2(5L_{AT})_{1/3}$

where $k_T = \frac{1}{5L_{AT}+1}$

$= \frac{Y_{bT}}{}$, $z = 1.48 + \sqrt{n}$ n Y ^{1} $^{0.2}$, $N_{bb} = 0.725(n)$, $N_{cb} = N_{bb}$

$_T$

$$\begin{pmatrix} R_{WCT} \\ G_{WCT} \\ B_{WCT} \end{pmatrix} = \begin{pmatrix} D_R R_{WT} \\ D_G G_{WT} \\ D_B B_{WT} \end{pmatrix}^{F} \quad (4)$$

$(\frac{LTRWCT}{})^{0.42}$

$$R_{aWT} = 400\left(\frac{F_L R_{WCT}(100)^{0.42}}{(100)^{0.42} + 27.13}\right) + 0.1 \quad (5)$$

Similarly, calculate the G_{aWT} and B_{aWT} by replacing R_{WCT} with G_{WCT} and B_{WCT}, respectively. Now, calculate the achromatic response for the white point using (7).

$A_{WT} = [2R_{aWT} + G_{aWT} + 0.05B_{aWT} - 0.305]N_{bb}$ (6) Apply the formulation (1)-(6) on the tone mapped image XYZ (X_T, Y_Y, Z_T) to get A_T as in (7).

$$A_T = [2R_{aT} + G_{aT} + 0.05B_{aT} - 0.305]N_{bb} \quad (7)$$

Finally, the lightness of the tone-mapped image is computed using (8).

$$J_T = 100\left(\frac{A_T}{A_{WT}}\right)^{c.z} \quad (8)$$ here c and z are the CIECAM16 default parameters.

Color Adaptation

The HDR images are given in linear domain and can be converted into XYZ (X_H, Y_H, Z_H) using the sRGB matrix or with the camera characterization model. The colors are adapted from HDR image under display surround conditions, i.e., L_{ad}, Y_{bd}. Hence, calculate the post adaption responses (R_{aH}, G_{aH}, B_{aH}) of the HDR image using (1)-(5), i.e.,

$(-F_{LHRCH}/100)^{0.42}$

$$R_{aH} = \begin{cases} -400\left(\frac{F_{LH}R_{CH}/100)^{0.42}}{(F_{LH}R_{CH}/100)^{0.42}+27.13}\right)+0.1, & R_{CH}<0 \\ \frac{(F_{LH}R_{CH}/100)^{0.42}}{(F_{LH}R_{CH}/100)^{0.42}+27.13}+0.1, & R_{CH}\geq 0 \end{cases} \quad (9)$$

The subscript H denotes the color are extracted from HDR image while the subscript d denotes that display surround parameters were used. Similarly, G_{aH} and B_{aH} can be calculated by replacing R_{CH} by G_{CH} and B_{CH}, respectively.

Calculate Hue Angle and Chroma

The hue angle can be calculated as follows.

$$b_H = \frac{12\cdot G_{aH} - B_{aH}}{R_{aH}+G_{aH}9-2B_{aH}} \quad (10)$$

$$h_c = \tan^{-1}(b_H/a_H) \quad (11)$$

$$a_H = R_{aH}11 - \frac{a_H}{11}$$

Finally, the new chroma is calculated using tone-mapped image lightness J_T and HDR image post adaptation equations as follows.

$$e_t = \frac{1}{4}\cdot\left[\cos\left(\frac{h_c\cdot\pi}{180}+2\right)+3.8\right]_1 \quad (12)$$

$$t = \frac{\left(\frac{50000}{13}\cdot N_c\cdot N_{cb}\right)\cdot e_t\cdot\left(a_H^2+b_H^2\right)^{1/2}}{R_{aH}+G_{aH}+\left(\frac{21}{20}\right)\cdot B_{aH}} \quad (13)$$

$$C_T = t^{0.9}\cdot\left(\frac{J_T}{100}\right)^{0.5}\cdot(1.64-0.29^n)^{0.73} \quad (14)$$

Now we have got hue h_c from the HDR image, the new Chroma C_T while using tone-mapped image lightness J_T. Note that other parameters N_c and N_{cb}, etc., are calculated using default CIECAM16 equations.

Display Image Transformation

In the previous steps, the perceptual hue h_c was restored from the HDR image and perceptual chroma C_T was calculated employing tone mapped image lightness J_t and CIECAM16 color adaptation equations to the HDR image. The perceptual correlates J_t C_T h_c can be transformed back to XYZ using display surround parameters and CIECAM16 inverse transformations. Subsequently, the display or the sRGB model may be used to calculate the display image. Since J_t is the original lightness in the color corrected image, it ensures the lightness preservation.

Following the recommendations of CIE Technical Report 159:2004, Luo *et al.* [13], the values of L_a and Y_b were selected. The tone mapped images are typically presented in sRGB color space hence to present the images here, D65 white point was used with $L_{aT} = L_{ad} = 100$ and $Y_{bT} = Y_{bd} = 20$, both in cd/m^2. Moreover, XYZ coordinates for the HDR images were obtained using a linear transformation from sRGB to XYZ.

Results and Discussion

Visual Comparisons and Discussions

Figure 3 (a) compares results of four CCMs, including CC$_z$. It is evident that Schlick's and Mantiuk's (automated versions) color corrected images (Li's TMO) result in significant desaturation in regions with high contrast changes as highlighted by rectangular areas. Since Artusi's method applies color desaturation step to out of gamut pixels, it is clear that Artusi's color corrected image is relatively low statured.

Figure 3 (b) displays an image tone-mapped using Li's TMO and color-corrected by four CCMs. It shows that the tone-mapped image has high saturation. Artusi's and Schlick's CCMs introduce lightness shifts and excessively desaturated colors. These lightness shifts are particularly noticeable in highlighted areas where objects appear too dark. For instance, the orange gourds in the original image are lighter compared to those in images processed by Artusi's and Schlick's methods.

Mantiuk's correction notably altered the hue of the orange colors. In contrast, CC$_z$ successfully preserves both the lightness and the hue, producing more vivid and optimal colors than the other CCMs.

Since CCz selectively adapts the colors from HDR images under surround conditions, it presents more accurate colors. The Figure 4 compares the tone mapped images using multiple TMOs and their color corrected versions by four CCMs, including CC$_z$. It can be noticed that the text "Waffle House" is flanked by light sources, both sides should appear less saturated, while the region under the text be more saturated. For true reproduction, this effect must be visible in the color corrected images. It can be noticed that other CCMs could not produce this differential effect and only CC$_z$ was able to reproduce the effect.

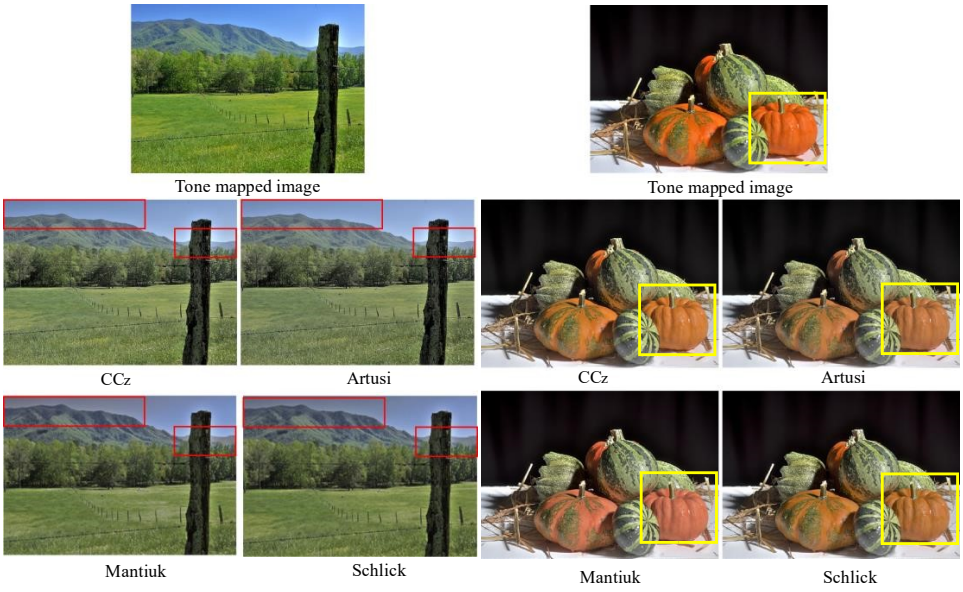

Figure 3. *(a) The Schlick and Mantiuk methods may suffer extreme desaturation for specific regions. (b): CC_z preserved lightness and restored original hue. Artusi's CCM altered the lightness darkening the image and overly desaturated the chroma. Schlick's CCM also distorted the lightness while Mantiuk's CCM distorted the hue.*

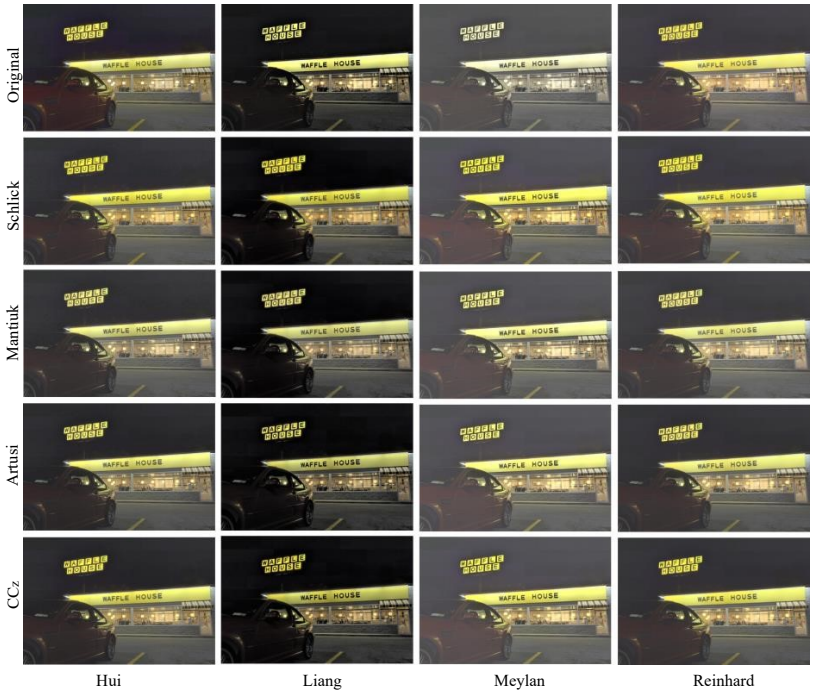

Figure 4: *Comparison of the proposed method with other CCMs employing various TMOs.*

Moreover, the images corrected by Artusi's method are overly desaturated. The color of the red car in Hui's image is selectively desaturated in CC_z, while the washed-out colors under the text "Waffle House" are a little enhanced to achieve the same effect. The image tone mapped with Reinhard's TMO [14] produced highly saturated colors in the entire image. The CC_z corrected the chroma, and the resultant image has adaptively less saturated colors in the car. It can be noted that the tone mapped image by Meylan TMO [23], was excessively desaturated with washed-out colors in the entire image. The CC_z reproduced the colors and the differential effect. Similar effects could be observed with images processed using Liang TMO.

Hue and Lightness differences

The color differences are generally calculated in the CIELAB color space; however, in CIELAB the hue is nonlinear in comparison to other color spaces such as CIECAM02 and CIECAM16. Therefore, the differences were evaluated using CIECAM16 perceptual attributes. In CC_z, the goal was to preserve the lightness of the tone-mapped image after color correction, restore the hue from the HDR image, and estimate a new chroma for the tone-mapped images. Consequently, lightness and hue differences were calculated in this analysis. Figure 5 shows the average lightness differences (ΔJ) and hue differences (Δh) for 104 images from the RIT database [15]. TMOs, such as Reinhard [14], Schlick [7], and Khan [16], share the same color preservation approach, so only Khan's TMO was included along with Hui [5], Liang [4], and Meylan [6] TMOs. Four TMOs and four color reproduction techniques were employed. The lightness differences of the color-corrected images were calculated against tone-mapped image, and hue differences were calculated against HDR images. Since hue is defined on a circle, Δh was determined as in (15) [9].

$$\Delta h = \min(|h_c - h_H|, \min(|h_c - h_H| + 2\pi + \max(|h_c - h_H|))) \quad (15)$$

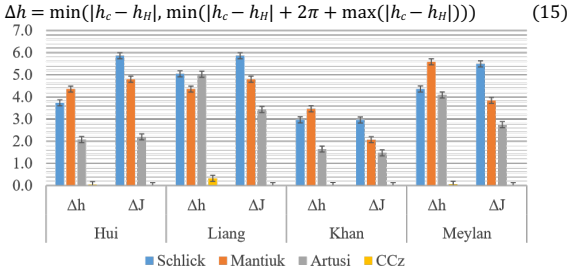

Figure 5: *Mean ΔJ and Δh of 104 color corrected images by employing CCMs. The error bars indicate 95% confidence interval.*

where h_c and h_H represent the hue of the color corrected and HDR images, respectively.

As shown in Figure 5, CC_z is consistent in preserving lightness and restoring hue, thus maintaining the same lightness in the color corrected image as in the tone mapped image. The minor differences observed are mainly due to the inaccuracy in the transformation equations. In contrast, other CCMs introduced shifts in lightness and hue, altering the lightness produced by the TMOs. These distortions are particularly prominent in Hui, Liang, and Meylan TMOs.

Psychophysical experiment

The lightness and hue differences can be measured objectively; however, since we aimed to reproduce chroma of the tone mapped image, the chroma accuracy cannot be measured objectively and we need to design a psychophysical experiment. A pair comparison-based experiment was conducted to compare the performance of CC_z with other models based on corrected chroma accuracy. In the previous studies, Mantiuk and Artusi used scaled versions of the HDR images as reference images in their psychophysical experiments. However, scaling HDR images itself is tone mapping process which in turn introduces color distortions in the reference images. Moreover, selecting images by few authors may also turn into biased results. The other scale used by authors is the overall preference of the images however it was reported that observers may prefer images with more colorfulness or saturation than the real senses [17]. Hence, in our psychophysical experiment, the naturalness scale was used to assess the models.

Experiment Design and Interface

Ten HDR images from the RIT database were used for tone mapping and color correction, as shown in Figure 6. These images included a variety of colors, featuring both night and natural scenes. The images were tone mapped using six TMOs including Hui, Liang, Khan, Meylan, Reinhard and Schlick TMOs using the default parameters. It was noted that Hui TMO produces relatively high saturation while Meylan TMO produces relatively low saturation. However, Reinhard TMO produces slightly over saturated images. Moreover, Liang TMO shifts the hue, Khan and Schick TMOs produce relatively high contrast images. Furthermore, Reinhard and Schlick TMOs were spatially invariant, while other TMOs were spatially variant. Hence, we selected a variety of TMOs to test the performance of the models Subsequently, each tone-mapped image was processed with four CCMs: Schick, Mantiuk, Artusi, and CC_z.

With 10 images, 6 TMOs, and 4 CCMs, there were 240 processed images and 360 comparison pairs. Each pair was repeated randomly to evaluate observer variation, resulting in 720 assessments per subject.

The images were displayed on an Apple Pro Display XDR in a dark room with a wall reflectance of approximately 4%. The peak luminance was set to CIE D65 white point and the CIE 1931 standard colorimetric observer at 562 cd/m². The calibration targets included a native color primaries aligned with the P3 color space. To evaluate spatial uniformity, the display was divided into 3x3 segments, yielding a mean CIELAB color difference (ΔE_{ab}) of 1.1. The gain-offset-gamma (GOG) display model was used for characterization, tested with 24 colors from the ColorChecker chart, resulting in an average ΔE_{ab} of 0.39, ranging from 0.16 to 1.13. The processed images were then transformed to display RGB using this model.

Subjects were required to pass the Ishihara color vision test before participating. Images were displayed in pairs, and the experimental interface is shown in Figure 7. Twenty observers participated in the experiment, ten each from Chinese and Pakistani ethnicities, including 8 females and 12 males, all students of Zhejiang University. The mean age was 26, with a maximum of 30 and an standard deviation (SD) of 2.8. A total of 14,400 assessments were collected.

Intra- and inter-observer variation was analyzed using the percentage of wrong decisions (WDs), where a WD occurred if an observer selected a different image on a repeated assessment. For intra-observer variability, the mean and SD of WDs were 18.72 and 9.07, respectively. For inter-observer variability, assessments were compared across subjects, resulting in mean and SD values of 22.23 and 9.6, respectively. These results indicate overall consistency within and between subjects, supporting the reliability of the findings.

Performance of CCMs

The raw scores were converted into standardized Z-scores [31], as shown in Figure 8, to compare the performance of four CCMs. Schlick's and Mantiuk's CCMs consistently scored lower

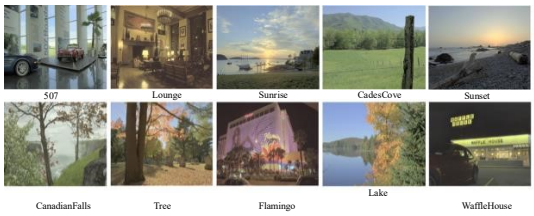

Figure 6: *The images used for the color correction psychophysical experiment.*

Figure 7: *The setup for the color correction psychophysical experiment.*

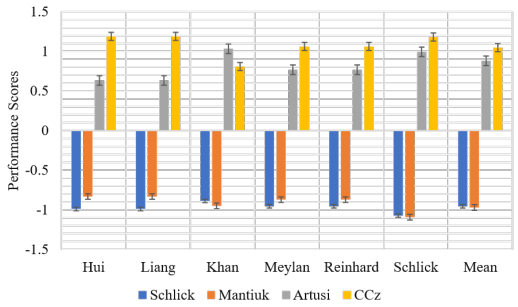

Figure:8 *Performance comparison of four CCMs using psychophysical results. The error bars indicate 95% confidence interval.*

than Artusi and CC_z across all TMOs, indicating less natural color reproduction. CC_z produced the most natural colors and generally outperformed other CCMs for five TMOs, except for Khan TMO where Artusi's method performed better. However, it was noted that Khan TMO produced higher contrast [17, 18] and Artusi CCM lowered the saturation as well as the lightness therefore the images were selected more by the subjects, however CC_z preserved original lightness but ranked lower due to over contrast produced by Khan TMO. Hui TMO required desaturation, while Meylan TMO required more saturation for color correction. For Reinhard, Khan, and Schlick TMOs the rankings of Artusi and CC_z were close. Since these three TMOs apply similar color preservation strategy during tone mapping therefore the behavior of these TMOs was similar in color correction. However, the mean scores of all the TMOs indicated that CC_z ranked higher among all the CCMs for each TMO as depicted in Figure 8.

Significance Tests

A significance test was conducted on the mean values of the rankings. Figure 9 depicts the results of multiple comparison significance test using ANOVA and Tukey's HSD criterion [19, 20]. This process involves two main steps: ANOVA analysis and multiple comparisons. ANOVA provides a p-value to determine if there is a significant difference in the means of groups i.e., TMOs. A p-value < 0.05 ($\alpha = 0.05$, 95% confidence interval)

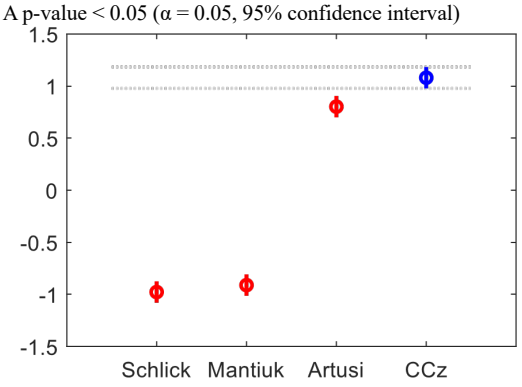

Figure 9: *Multiple comparison significance tests using ANOVA and Tukey's HSD criterion. The CCMs having intervals not intersecting with other CCMs are significantly different.*

indicates significance between the TMOs. Afterward, the multiple comparisons are performed using a post-hoc method such as the Tukey's HSD criterion test, which identifies critical values for each pairwise comparison among groups [19, 21]. The critical values determine if the difference between the means of the two groups (CCMs) is significant. If the calculated difference is greater than the critical value, the difference is considered significant and the null hypothesis is rejected. In Figure 9, the CCMs means are significantly different if their intervals do not coincide. The interval for Schlick and Mantiuk CCMs coincide, which mean Schlick and Mantiuk color corrected images were not significantly different. Moreover, Schlick and Mantiuk CCMs intervals do not intersect with the CC_z and Artusi CCMs. It is due to the fact the images of Artusi and CC_z were preferred more when compared to the color-corrected images by Schlick and Mantiuk CCMs. It implies that Artusi and CC_z were significantly different than Schlick and Mantiuk CCMs. Moreover, the intervals of none of the CCM including Artusi coincide with the interval of the CC_z therefore CC_z is significantly different from other CCMs. It can be noted from Figure 8 that CC_z ranked higher than other CCMs and Figure 9 suggests that CC_z was significantly different from other CCMs. Hence, it can be concluded that CC_z was significantly better than other CCMs in terms of natural color reproduction.

Conclusions

Adaptive chroma correction model CC_z was proposed to address color distortions in tone mapping. The input to the CC_z consisted of the tone mapped image and the corresponding original HDR image in linear RGB color space without any processing. The lightness of the tone mapped image was computed using CIECAM16 and tone mapped image surround conditions. Afterward, the hue and chroma were computed from the HDR image by employing tone mapped image lightness and CIECAM16 color adaptation equations of the HDR image under display surround conditions.

Since in CC_z, original lightness and hue were restored therefore the lightness and hue differences were lowest compared to the other CCMs. The visual comparisons and psychophysical experiments showed that CC_z produced the most natural colors among other CCMs and was ranked significantly better. The proposed model can be applied to any TMO whether spatially

variant or invariant making it effective post processing technique for the TMOs.

References

[1] N. Zhang, Y. Ye, Y. Zhao, X. Li, and R. Wang, "Fast and flexible stack-based inverse tone mapping," *CAAI Transactions on Intelligence Technology,* 2023.

[2] Y. Vinker, I. Huberman-Spiegelglas, and R. Fattal, "Unpaired learning for high dynamic range image tone mapping," in *Proceedings of the IEEE/CVF international conference on computer vision*, pp. 14657-14666, 2021.

[3] Y. Li, L. Sharan, and E. H. Adelson, "Compressing and companding high dynamic range images with subband architectures," *ACM transactions on graphics (TOG),* vol. 24, no. 3, pp. 836-844, 2005.

[4] Z. Liang, J. Xu, D. Zhang, Z. Cao, and L. Zhang, "A hybrid l1-l0 layer decomposition model for tone mapping," in *Proceedings of the IEEE conference on computer vision and pattern recognition*, pp. 4758-4766, 2018.

[5] H. Li, X. Jia, and L. Zhang, "Clustering based content and color adaptive tone mapping," *Computer Vision and Image Understanding,* vol. 168, pp. 37-49, 2018.

[6] L. Meylan and S. Susstrunk, "High dynamic range image rendering with a retinex-based adaptive filter," *IEEE Transactions on image processing,* vol. 15, no. 9, pp. 2820-2830, 2006.

[7] C. Schlick, "Quantization techniques for visualization of high dynamic range pictures," in *Photorealistic rendering techniques*: Springer, 1995, pp. 7-20.

[8] R. Mantiuk, R. Mantiuk, A. Tomaszewska, and W. Heidrich, "Color correction for tone mapping," in *Computer Graphics Forum*, pp. 193-202, 2009.

[9] A. Artusi, T. Pouli, F. Banterle, and A. O. Akyüz, "Automatic saturation correction for dynamic range management algorithms," *Signal Processing: Image Communication,* vol. 63, pp. 100-112, 2018.

[10] N. Moroney, M. D. Fairchild, R. W. Hunt, C. Li, M. R. Luo, and T. Newman, "The CIECAM02 color appearance model," in *Color and Imaging Conference*, pp. 23-27, 2002.

[11] C. Li *et al.*, "Comprehensive color solutions: CAM16, CAT16, and CAM16UCS," *Color Research & Application,* vol. 42, no. 6, pp. 703-718, 2017.

[12] M. Safdar, J. Y. Hardeberg, and M. R. Luo, "ZCAM, a colour appearance model based on a high dynamic range uniform colour space," *Optics Express,* vol. 29, no. 4, pp. 6036-6052, 2021.

[13] M. R. Luo and C. Li, "CIECAM02 and its recent developments," *Advanced color image processing and analysis,* pp. 19-58, 2013.

[14] E. Reinhard, M. Stark, P. Shirley, and J. Ferwerda, "Photographic tone reproduction for digital images," in *Proceedings of the 29th annual conference on Computer graphics and interactive techniques*, pp. 267-276, 2002.

[15] M. D. Fairchild, "The HDR photographic survey," in *Color and imaging conference*, pp. 233-238, 2007.

[16] I. R. Khan, S. Rahardja, M. M. Khan, M. M. Movania, and F. Abed, "A tonemapping technique based on histogram using a sensitivity model of the human visual system," *IEEE Transactions on Industrial Electronics,* vol. 65, no. 4, pp. 3469-3479, 2017.

[17] I. Mehmood, X. Liu, M. U. Khan, and M. R. Luo, "Method for developing and using high quality reference images to evaluate tone mapping operators," *JOSA A,* vol. 39, no. 6, pp. B11-B20, 2022.

[18] I. Mehmood, X. Shi, M. U. Khan, and M. R. Luo, "Perceptual Tone Mapping Model for High Dynamic Range Imaging," *IEEE Access,* 2023.

[19] Y. Hochberg and A. C. Tamhane, *Multiple comparison procedures*. John Wiley & Sons, Inc., 1987.

[20] T. K. Kim, "Understanding one-way ANOVA using conceptual figures," *Korean journal of anesthesiology,* vol. 70, no. 1, pp. 22-26, 2017.

[21] G. A. Milliken and D. E. Johnson, *Analysis of messy data volume 1: designed experiments*. CRC Press, 2009.